JACS
JOURNAL OF THE AMERICAN CHEMICAL SOCIETY
Communication
pubs.acs.org/JACS

Rapid Heteronuclear Single Quantum Correlation NMR Spectra at Natural Abundance

David Schulze-Sünninghausen, Johanna Becker, and Burkhard Luy*

Institut für Organische Chemie and Institut für Biologische Grenzflächen, Karlsruher Institut für Technologie (KIT), Fritz-Haber-Weg 6, 76131 Karlsruhe, Germany

ABSTRACT: A novel NMR experiment, the so-called ASAP-HSQC, is introduced that allows the detection of heteronuclear one-bond correlations in less than 30 s on small molecules at natural abundance without compromises in sweep width, resolution or spectral quality. Equally, the experiment allows a significant increase in digital resolution or a moderate senstitivity enhancement in the same overall experiment time compared to a conventional HSQC. The gain is a consequence of keeping all unused proton magnetization along z during acquisition, so that the previously reported ASAP and ALSOFAST approaches can be transferred from HMQC to HSQC-type experiments. Next to basic and broadband pulse sequences, a characterization of the sequence with respect to minimum measurement time, sensitivity gain, and advantages in resolution compared to state-of-the-art experiments is given.

High-resolution 2D NMR-spectroscopy is an essential tool to chemists of all trades to identify, quantify, and correlate molecules in solution. Especially heteronuclear correlation experiments, like the HSQC (heteronuclear single quantum correlation spectroscopy[1]), contain a wealth of information and allow resolution of crowded spectral regions due to the dispersion in the additional dimension.

Two main problems remain with the application of such spectra: the overall low sensitivity inherent to NMR spectroscopy that is intensified with low natural abundance nuclei, such as ^{13}C or ^{15}N, and the overall experiment time necessary to acquire the large number of increments of a 2D data set even if the sample provides sufficient sensitivity. The latter limitation is, for example, very critical for the observation of intermediate reaction or folding products or for highly repetitive applications such as quality control or metabolomics-type studies. As a consequence, a large number of experimental modifications have been developed during the last decades.

Ultrafast experiments today are able to acquire a 2D experiment in a single scan using gradient-encoding imaging-type schemes.[2] The acquisition scheme, however, poses severe limits in accessible resolution and sweep width due to diffusion and available gradient strengths. More conventional, less restrictive methods either allow the acquisition of a reduced data set by applying special processing techniques,[3] or shorten the experimental time needed per scan, usually by decreasing the recovery delay. The most widely used method in this context is the famous Ernst angle,[4] which in most cases can be combined with other techniques as for example the SOFAST-HMQC,[5] extended flip-back schemes,[6] the BEST approach,[7] the ASAP-HMQC,[8a] the SMART approach,[9] or slice-selective excitation.[10]

In our hands, the ASAP-HMQC (acceleration by sharing adjacent polarization heteronuclear multiple quantum correlation spectroscopy) gives the maximum enhancement for small molecules at natural abundance and on the basis of its principles we propose in the following the ASAP-HSQC as a very fast 2D heteronuclear correlation experiment with uncompromised spectral quality that can be applied the same way as a conventional HSQC experiment.

The ASAP-HMQC[8a] excites selectively all ^{13}C-bound protons, while positioning all other protons along z, providing the polarization for the following scan. This reservoir of polarization is then simply exchanged with the ^{13}C-bound protons via a short homonuclear isotropic mixing period of approximately 40 ms without additional recovery delay. Although it is well-known that the HSQC experiment provides better spectral quality as an HMQC experiment,[19] a corresponding ASAP experiment has not been reported yet. The reason is that a conventional implementation of the HSQC, using coherence order selection and echo/antiecho acquisition as shown for example in Figure 1A, leads to dephasing of magnetization of protons not directly attached to ^{13}C nuclei and therefore makes it impossible to store the required polarization for the next scan. In Figure 1B, instead, an ASAP-HSQC is shown with a modified gradient scheme that retains the polarization reservoir for all the passive spins not directly bound to the NMR-active heteronucleus. The main difference is the application of the 90° pulse of the back-transfer step with $-x$ phase *before* the actual coherence order selection and echo/antiecho encoding (Figure 1). This way the polarization reservoir is flipped along z, ensuring that it is not affected by the gradients. Coherence order selection is then achieved by dephasing either zero quantum or double quantum coherences with a gradient G_5 before the desired single quantum coherence is refocused using $G_6 = G_5\ (1-\gamma_H/\gamma_C)$ or $G_6 = G_5\ (1+\gamma_H/\gamma_C)$, respectively.

For the practical implementation of the ASAP-HSQC of Figure 1B we used DIPSI-2[17] as a well-known isotropic mixing sequence and broadband BEBOP,[12] BURBOP,[13,15] and BUBI[14] shaped pulses for improved robustness and sensitivity as described in more detail in the figure caption. Ernst-angle type excitation was achieved by optimizing the delay Δ' as reported for the ALSO-FAST HMQC.[20] The implementation of this approach ensures a sensitivity enhancement even for a spin

Received: November 13, 2013
Published: January 13, 2014

dx.doi.org/10.1021/ja411588d | J. Am. Chem. Soc. 2014, 136, 1242−1245

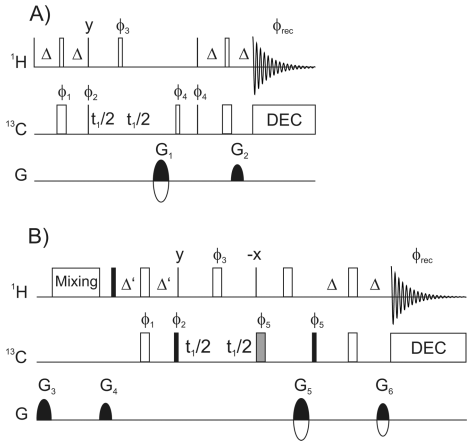

Figure 1. Pulse sequences for a conventional HSQC (A) and the ASAP-HSQC (B). Pulse phases are x unless indicated otherwise. Vertical lines represent 90° hard pulses, thin open boxes 180° hard pulses. In (A) wider open boxes indicate CHIRP inversion pulses[11] of 500 μs duration. In (B) the filled box on ^{1}H marks a BEBOP(10 kHz, 20 kHz, 550 μs, ± 20%, 1100)[12] pulse using the nomenclature introduced in,[13] the pairs of ^{1}H/^{13}C open boxes during INEPT transfer steps represent 600 μs BUBI pulse sandwiches,[14] where the proton pulse is also used as a BURBOP-180$_x$(10 kHz, 20 kHz, 600 μs, ± 20%, 1200)[13,15] refocusing pulse for the other open boxes. The gray shaded ^{13}C refocusing pulse after t_1 evolution is a BURBOP-180$_y$ (37.5 kHz, 10 kHz, 1.1 ms, ± 5%, 2200). All proton shaped pulses are applied with an rf-amplitude of 20 kHz, while it is 10 kHz for carbon shapes. Although only a subset has been used for the experiments shown, full phase cycling is given by $\phi_1 = x$; $\phi_2 = x,-x$; $\phi_3 = 2(x),2(-x)$; $\phi_4 = 4(x),4(-x)$; $\phi_5 = 4(-x),4(x)$; $\phi_{rec} = x,-x,x,-x,-x,x,-x,x$. The delay $\Delta = 1/(2\,{}^1J_{CH})$ is typically set to an average coupling constant of 145 Hz, while Δ' is optimized individually for every sample. $\Delta' = 1.2$ ms and $\Delta' = 1.3$ ms, respectively, was used for menthol and maltose spectra shown in this article. Heteronuclear decoupling was achieved using GARP.[16] Isotropic mixing in between scans in (B) was performed using the DIPSI-2 sequence.[17] Purge gradients were set to $G_3 = 43\%$ and $G_4 = 33\%$ of the maximum gradient strength of 50.7 G/cm, while echo/antiecho and coherence order selection was achieved by switching gradients according to $G_1 = (80\%,-80\%)$, $G_2 = (20.1\%,20.1\%)$ or $G_5 = (63.9\%,80\%)$, $G_6 = (80\%,59.9\%)$ every other increment. TPPI-like incrementation[18] with the echo/antiecho recording scheme was achieved by simultaneous inversion of phases ϕ_1 and ϕ_2.

system which contains only isolated CH-groups. Example spectra were recorded on 500 mM menthol in $CDCl_3$, or 200 mM maltose in D_2O using a 600 MHz Bruker Avance III spectrometer equipped with a ^{1}H,^{13}C,^{15}N-TCI inversely detecting cryoprobe at 300 K. A DIPSI-2 isotropic mixing period of 34.53 ms was irradiated between consecutive scans.

With shortened interscan delays and acquisition times of 107 ms for the FID, an ASAP-HSQC can be recorded in less than 30 s as is shown in Figure 2. The spectral quality is basically identical to a conventional HSQC spectrum. On the other hand, the fast acquisition of spectra allows the averaging over many more scans for the same overall experiment time. In Figure 3 a conventional HSQC sequence with a recycle delay of 2 s, i.e. slightly shorter than corresponding T_1-times of the menthol sample used, and an overall experiment time of 9 min and 34 s is compared to an ASAP-HSQC of slightly shorter overall duration. Clearly, a moderate gain in sensitivity is visible throughout the ASAP-HSQC, given by an increase of 3−4 in intensity with simultaneously increased noise of $\sqrt{7}$ due to the seven times enlarged number of scans. The overall spectral

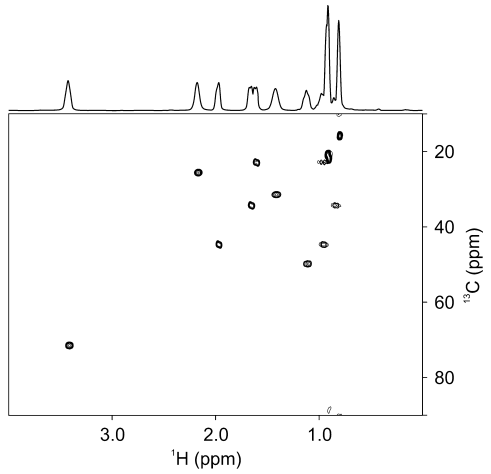

Figure 2. The ASAP-HSQC optimized for rapid 2D detection applied to menthol in $CDCl_3$. The spectrum was recorded using 512 × 128 data points with spectral widths of 2398 and 12064 Hz (corresponding to acquisition times of 106.8 and 5.3 ms) and one scan per t_1 increment and 16 dummy scans. The overall experiment time was 28 s.

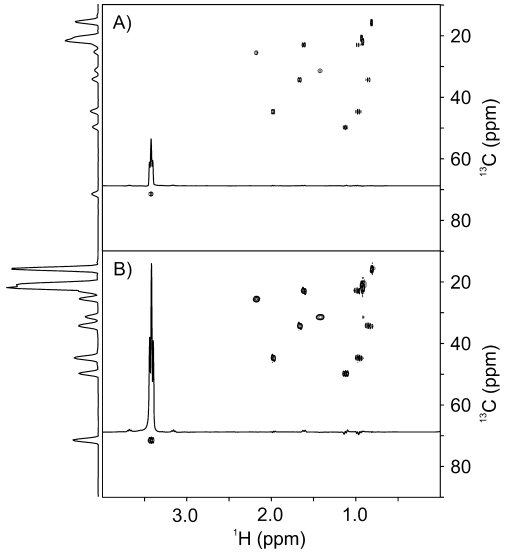

Figure 3. Comparison of a conventional HSQC and an ASAP-HSQC of menthol in $CDCl_3$ with equivalent overall measurement time. Both spectra were recorded with 1024 × 128 complex data points, corresponding to acquisition times of 213.5 and 5.3 ms for the two dimensions. For the conventional HSQC, 2 scans per t_1 increment and four dummy scans with a recovery delay of 2 s close to the average T_1 times were applied, which results in a measurement time of 9 min and 34 s (A). The ASAP HSQC was acquired using 14 scans per t_1 increment and 16 dummy scans in 9 min and 17 s (B). While spectral quality is identical, a relative increase in intensity of 3−4 is observed for the ASAP-HSQC with an simultaneous increase in noise of only $\sqrt{7}$.

quality is equal or even slightly improved with less artifacts in the ASAP-HSQC compared to the conventional HSQC.

The full potential of the ASAP-HSQC in terms of resolution is shown in Figure 4: due to the fast acquisition scheme it is now possible to acquire a large number of increments in a reasonable experiment time, so that for example 512 (^{1}H) × 16384 (^{13}C) data points could be acquired in slightly more than 3 h. With the resulting digital resolution after zero filling of 0.55

dx.doi.org/10.1021/ja411588d | J. Am. Chem. Soc. 2014, 136, 1242−1245

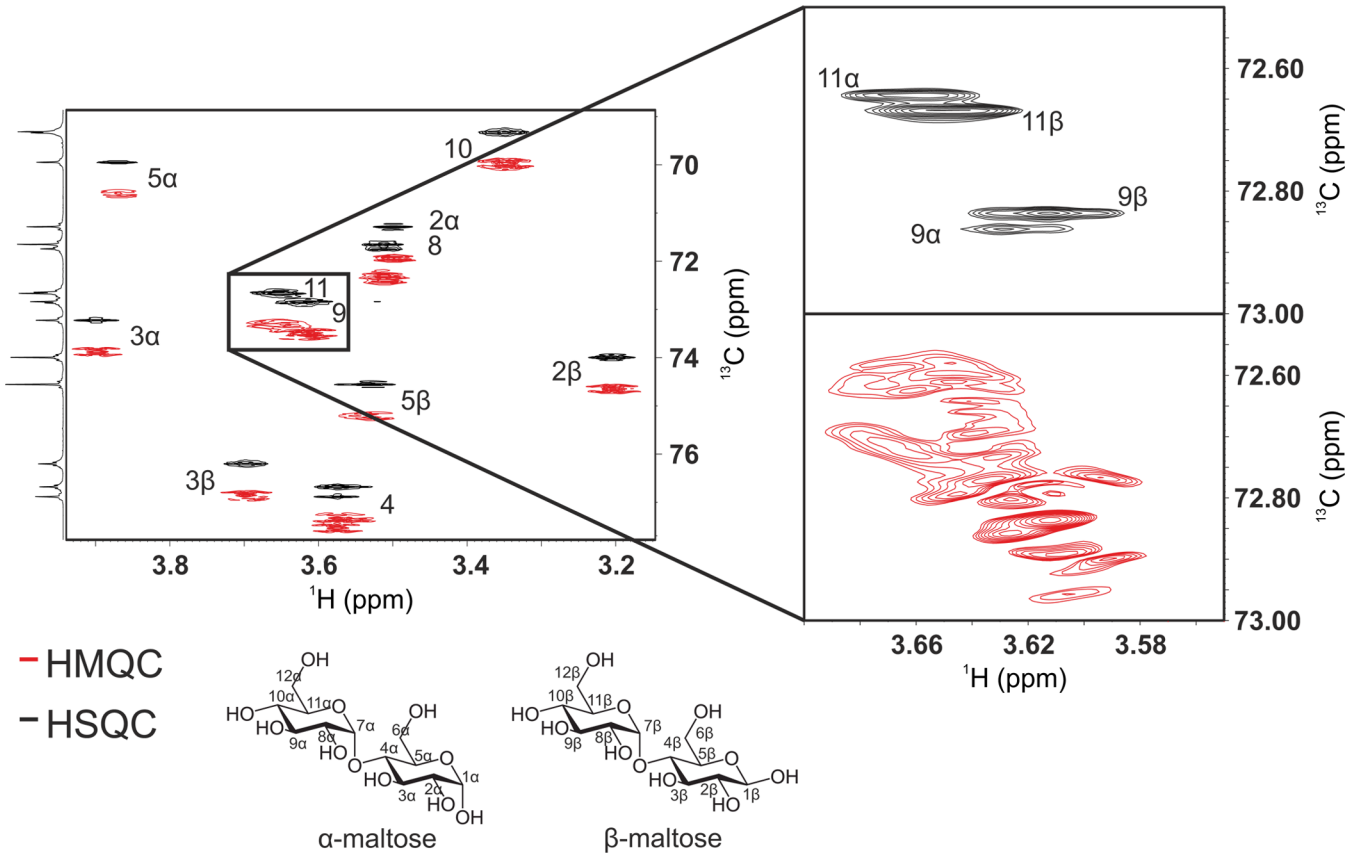

Figure 4. Comparison of ASAP-HSQC and ASAP-HMQC spectra acquired on maltose in D_2O. Both spectra were recorded with a large number of t_1 increments, i.e. 512 (^{1}H) × 16384 (^{13}C) complex data points and acquisition times of 142.3 and 905.4 ms. This corresponds to a digital resolution of 0.55 Hz in the carbon dimension after zero filling to 32768 points. One scan per t_1 increment and 16 dummy scans were acquired in 3 h, 6 min, and 37 s for the ASAP-HSQC, and in 3 h, 7 min, and 10 s for the ASAP-HMQC. Clearly the advantage in resolution can be seen, which even allows the distinction of 9α/β and 11α/β of maltose, which are each approximately 3 Hz apart.

Hz all cross peaks of maltose can be clearly resolved - even carbons 9 and 11 of the α- and β-form of the disaccharide can be distinguished easily. The ASAP-HMQC, instead, shows broad fuzzy multiplets in the indirect dimension due to evolution of multiple quantum coherences, which prohibits the distinction of such signals.

In summary, the presented ASAP-HSQC allows acquisition of uncompromised HSQC spectra with drastically reduced recovery delays in between scans for small molecules at natural abundance. Compared to conventional HSQC experiments this can lead to reduced overall experiment time, enhanced sensitivity, or higher digital resolution in the carbon dimension. The reduction of measurement time or increase in resolution might be even further improved by the additional use of nonuniform sampling techniques. The improvements will be beneficial for a wide range of small molecule applications at no additional costs.

AUTHOR INFORMATION

Corresponding Author

Burkhard.Luy@kit.edu

Notes

The authors declare no competing financial interest.

ACKNOWLEDGMENTS

B.L. thanks the Deutsche Forschungsgemeinschaft (LU 835/4,7,8; Forschergruppe FOR 934 and DFG-Gerätezentrum Pro^{2}NMR), the Fonds der Chemischen Industrie, and the HGF programme BioInterfaces.

REFERENCES

(1) Bodenhausen, G.; Ruben, D. J. *Chem. Phys. Lett.* **1980**, *69*, 185−189.

(2) (a) Frydman, L.; Scherf, T.; Lupulescu, A. *Proc. Natl. Acad. Sci. U.S.A.* **2002**, *99*, 15858−15862. (b) Pelupessy, P. *J. Am. Chem. Soc.* **2003**, *125*, 12345−12350. (c) Tal, A.; Frydman, L. *Prog. Nucl. Magn. Reson. Spectrosc.* **2010**, *57*, 241−292.

(3) (a) Brüschweiler, R.; Zhang, F. L. *J. Chem. Phys.* **2004**, *120*, 5253−5260. (b) Kupče, Ē.; Freeman, R. *J. Am. Chem. Soc.* **2004**, *126*, 6429−6440. (c) Mandelshtam, V. A.; Taylor, H. S.; Shaka, A. J. *J. Magn. Reson.* **1998**, *133*, 304−312. (d) Schmieder, P.; Stern, A. S.; Wagner, G.; Hoch, J. C. *J. Biomol. NMR* **1993**, *3*, 569−576. (e) Orekhov, V. Y.; Jaravine, V. A. *Prog. Nucl. Magn. Reson. Spectrosc.* **2011**, *59*, 271−292. (f) Holland, D. J.; Bostock, M. J.; Gladden, L. F.; Nietlispach, D. *Angew. Chem., Int. Ed.* **2011**, *50*, 6548−6551.

(4) Ernst, R. R.; Bodenhausen, G.; Wokaun, A., *Principles of Nuclear Magnetic Resonance in One and Two Dimensions*; Oxford University Press: New York, 1987.

(5) (a) Schanda, P.; Brutscher, B. *J. Am. Chem. Soc.* **2005**, *127*, 8014−8015. (b) Schanda, P.; Kupče, Ē.; Brutscher, B. *J. Biomol. NMR* **2005**, *33*, 199−211. (c) Kern, T.; Schanda, P.; Brutscher, B. *J. Magn. Reson.* **2008**, *190*, 333−338.

(6) Diercks, T.; Daniels, M.; Kaptein, R. *J. Biomol. NMR* **2005**, *33*, 243−259.

(7) (a) Schanda, P.; Van Melckebeke, H.; Brutscher, B. *J. Am. Chem. Soc.* **2006**, *128*, 9042−9043. (b) Lescop, E.; Schanda, P.; Brutscher, B. *J. Magn. Reson.* **2007**, *187*, 163−169.

(8) (a) Kupče, Ē.; Freeman, R. *Magn. Reson. Chem.* **2007**, *45*, 2−4. (b) Furrer, J. *Chem. Commun.* **2010**, *46*, 3396−3398.
(9) Vitorge, B.; Bodenhausen, G.; Pelupessy, P. *J. Magn. Reson.* **2010**, *207*, 149−152.
(10) Wagner, G. E.; Sakhaii, P.; Bermel, W.; Zangger, K. *Chem. Commun.* **2013**, *49*, 3155−3157.
(11) Bohlen, J. M.; Burghardt, I.; Rey, M.; Bodenhausen, G. *J. Magn. Reson.* **1990**, *90*, 183−191.
(12) (a) Kobzar, K.; Skinner, T.; Khaneja, N.; Glaser, S.; Luy, B. *J. Magn. Reson.* **2004**, *170*, 236−243. (b) Kobzar, K.; Skinner, T. E.; Khaneja, N.; Glaser, S. J.; Luy, B. *J. Magn. Reson.* **2008**, *194*, 58−66. (c) Skinner, T.; Kobzar, K.; Luy, B.; Bendall, M.; Bermel, W.; Khaneja, N.; Glaser, S. *J. Magn. Reson.* **2006**, *179*, 241−249. (d) Skinner, T.; Reiss, T.; Luy, B.; Khaneja, N.; Glaser, S. *J. Magn. Reson.* **2003**, *163*, 8−15. (e) Skinner, T.; Reiss, T.; Luy, B.; Khaneja, N.; Glaser, S. *J. Magn. Reson.* **2004**, *167*, 68−74.
(13) Kobzar, K.; Ehni, S.; Skinner, T. E.; Glaser, S. J.; Luy, B. *J. Magn. Reson.* **2012**, *225*, 142−160.
(14) (a) Ehni, S.; Luy, B. *Magn. Reson. Chem.* **2012**, *50*, S63−S72. (b) Ehni, S.; Luy, B. *J. Magn. Reson.* **2013**, *232*, 7−17.
(15) (a) Luy, B.; Kobzar, K.; Skinner, T.; Khaneja, N.; Glaser, S. *J. Magn. Reson.* **2005**, *176*, 179−186. (b) Skinner, T. E.; Gershenzon, N. I.; Nimbalkar, M.; Bermel, W.; Luy, B.; Glaser, S. J. *J. Magn. Reson.* **2012**, *216*, 78−87.
(16) Shaka, A. J.; Barker, P. B.; Freeman, R. *J. Magn. Reson.* **1985**, *64*, 547−552.
(17) Shaka, A. J.; Lee, C. J.; Pines, A. *J. Magn. Reson.* **1988**, *77*, 274−293.
(18) Marion, D.; Wüthrich, K. *Biochem. Biophys. Res. Commun.* **1983**, *113*, 967−974.
(19) Bax, A.; Ikura, M.; Kay, L. E.; Torchia, D. A.; Tschudin, R. *J. Magn. Reson.* **1990**, *86*, 304−318.
(20) Mueller, L. *J. Biomol. NMR* **2008**, *42*, 129−137.